Proceedings of the 15th International Conference on Manufacturing Systems – ICMaS
Published by Editura Academiei Române, ISSN 1842-3183

"Politehnica" University of Bucharest, Machine and Manufacturing Systems Department
Bucharest, Romania, 26–27 October, 2006

A PARAMETRIC MODEL OF THE INVERSE DYNAMICS FOR THE 3-PUU CLASS OF PURE TRANSLATIONAL PARALLEL MANIPULATORS

Marco PRINCIPI

Abstract: *This paper introduces a parametric formulation of the inverse dynamics problem for the pure translational 3-PUU parallel architecture, aimed to provide a forecast of the solicitations on the mechanic structure and a survey over its stiffness capability to be implemented into an optimization study. The elaborated algorithms were collected in a MATLAB® toolbox and verified by mean of the CAE multibody analysis software MSC visualNastran®.*

Key words: *pure translational PKM, parametric model of dynamics, 3-PUU, resistance ellipsoids.*

1. INTRODUCTION

This paper introduces a parametric formulation of the inverse dynamics and stiffness analysis for the pure translational 3-PUU parallel architecture, developed as a MATLAB® procedure with the aim of providing a tool for the simultaneous optimization of both the aspects of such architecture.

The correspondence of this model was positively verified by mean of the multibody analysis software MSC VisualNastran.

A 3-PUU parallel robot (Fig. 1) has three identical and symmetric branches: each of them is made up of a slider that is connected to the frame by a synchronous linear motor that is modeled as an actuated prismatic joint, and a leg that is connected to the slider and to the mobile platform respectively by the upper and the lower universal joints. Under the condition that the two couples of vectors representing the rotational degrees of freedom left by the lower and the upper universal joint of the same leg coincide and are independent from those of the other two legs, this mechanism allows only the pure translational motion of the tool platform [5].

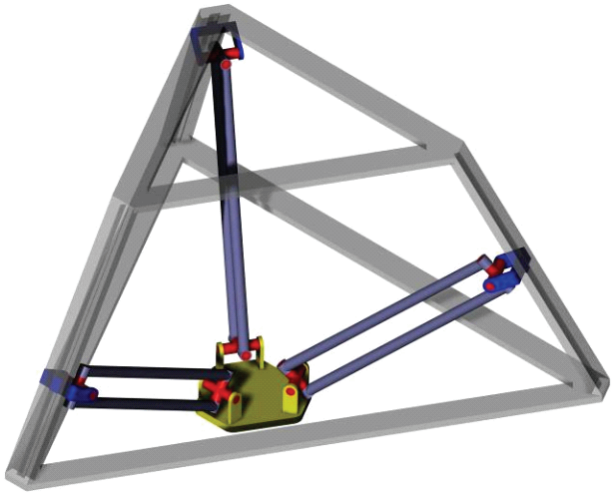

Fig. 1. A 3-PUU robotic platform.

2. THE KINEMATIC MODEL

The geometric parameters that can be manipulated in the multi-object optimization process are the radii of the platform's fixed and mobile platform, the length of the struts and the slope ϕ of the linear drives on the fixed platform, that coincide with the edges of a tetrahedron, whose vertex shifts towards the infinity as long as the fixed columns are close to verticality or falls on the same plane containing the linear drives, if they are arranged in a horizontal layout (see Fig. 2). Both the limit values of the slope call for specific solving algorithms of the position problem; on the other hand the differential and dynamic analysis algorithm fits all arrangements.

Referring to Fig. 3, we identify:

- **a**, **b**, **c** are placed at the center of the lower universal joints. They are inscribed in a circle with radius **r**;
- **P** is the projection of the TCP upon such triangle;
- The directions along which the centers of the upper universal joints **A**, **B**, **C** move are $\hat{\mathbf{A}}$, $\hat{\mathbf{B}}$, $\hat{\mathbf{C}}$. They intersect the upper base of the fixed frame on $\mathbf{A_1}$, $\mathbf{B_1}$, $\mathbf{C_1}$, that are inscribed in a circle whose radius is *R*. Similarly, $\mathbf{A_0}$, $\mathbf{B_0}$, $\mathbf{C_0}$, are the intersections with the plane that instantaneously contains points **a**, **b**, and **c**;
- The unit vectors $\hat{\mathbf{a}}$, $\hat{\mathbf{b}}$, $\hat{\mathbf{c}}$ describe the orientations of the mobile legs. Their length is *L*;
- α, β, γ are the angles between the projections of the fixed columns and corresponding legs upon the plane through **a**, **b**, and **c**;

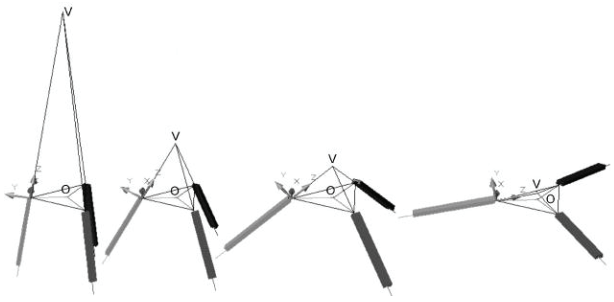

Fig. 2. Fixed frames with different slopes of the linear drives.

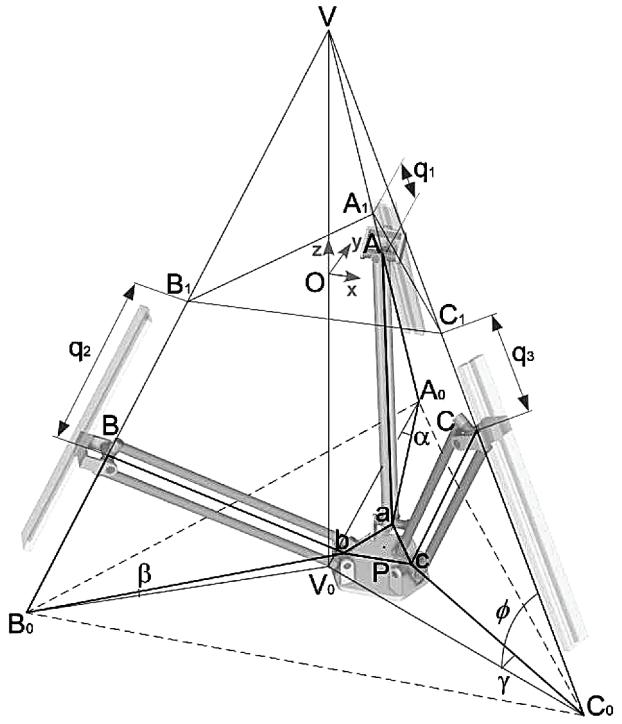

Fig. 3. The parametric kinematic model of a 3-PUU platform.

2.1. Inverse position analysis

The position of the mobile platform is identified by three independent kinematical chains, made up by the polygons **PVAa**, **PVBb** and **PVCc**. In a further detail the distances between points **A**, **B**, **C** and $\mathbf{A_1}$, $\mathbf{B_1}$, $\mathbf{C_1}$, measured by the independent coordinates q_1, q_2, q_3 are:

$$\begin{aligned} q_1 &= \frac{|\mathbf{VV_0}|-R}{\sin\phi_1} - |aA_0|\cos\phi_1 - \sqrt{L^2 - |aA_0|^2\sin^2\phi_1} \\ q_2 &= \frac{|\mathbf{VV_0}|-R}{\sin\phi_2} - |bB_0|\cos\phi_2 - \sqrt{L^2 - |bB_0|^2\sin^2\phi_2} \\ q_3 &= \frac{|\mathbf{VV_0}|-R}{\sin\phi_3} - |cC_0|\cos\phi_3 - \sqrt{L^2 - |cC_0|^2\sin^2\phi_3}. \end{aligned} \quad (1)$$

The relations between angles ϕ_1, ϕ_2, ϕ_3 and α, β, γ are:

$$\begin{aligned} &\cos\phi_1 = \cos\phi\cos\alpha; \quad \alpha = \mathrm{ATAN2}(a_x - A_{0x}; a_y - A_{0y}) \\ &\cos\phi_2 = \cos\phi\cos\beta; \quad \beta = \mathrm{ATAN2}(b_y - B_{0y}; b_x - B_{0x}) - \pi/6 \\ &\cos\phi_3 = \cos\phi\cos\gamma; \quad \gamma = \mathrm{ATAN2}(c_y - C_{0y}; c_x - C_{0x}) - 5\pi/6. \end{aligned} \quad (2)$$

2.2. Singular arrangements of the fixed frame

The equations (1) fail to describe the architectures with vertical or horizontal prismatic pairs. In the first case the problem is solved by replacing $|\mathbf{VV_0}|$, that rises infinitely, with $|\mathbf{OV_0}|$; in the latter, where $\phi = 0$, the vertex of the mobile platform lays on three circles with the centers in **A**, **B** and **C** and radius L_0, that is to say the projection of the struts over the plane containing the fixed platform. The correctness of this assumption was verified by checking the convergence of its results with those one of a quasi-horizontal, but not singular, layout.

2.3. Forward velocity analysis

First of all, we want to express the angular velocities of the legs in terms of the linear velocities $\dot{q}_1$, $\dot{q}_2$, $\dot{q}_3$ of the actuated prismatic joints A, B, C along their respective motion directions $\hat{\mathbf{A}}$, $\hat{\mathbf{B}}$, $\hat{\mathbf{C}}$.

Due to the pure-translational motion of the mobile platform, the centers of the three lower universal joints have the same velocity:

$$\begin{cases} \dot{q}_1 \cdot \hat{\mathbf{A}} + \boldsymbol{\omega}_A \times l\hat{\mathbf{a}} = \dot{q}_2 \cdot \hat{\mathbf{B}} + \boldsymbol{\omega}_B \times l\hat{\mathbf{b}} \\ \dot{q}_2 \cdot \hat{\mathbf{B}} + \boldsymbol{\omega}_B \times l\hat{\mathbf{b}} = \dot{q}_3 \cdot \hat{\mathbf{C}} + \boldsymbol{\omega}_C \times l\hat{\mathbf{c}}. \end{cases} \quad (3)$$

That are the linear system of six equations in nine unknown Cartesian components of the angular velocities of legs. The three missing equations come from the mutual arrangements of the universal joints on each leg, that prevent any rotation around their common axes.

$$L \cdot \begin{vmatrix} 0 & \hat{a}_z & -\hat{a}_y & 0 & -\hat{b}_z & \hat{b}_y & 0 & 0 & 0 \\ -\hat{a}_z & 0 & \hat{a}_x & \hat{b}_z & 0 & -\hat{b}_x & 0 & 0 & 0 \\ \hat{a}_y & -\hat{a}_x & 0 & -\hat{b}_y & \hat{b}_x & 0 & 0 & 0 & 0 \\ 0 & 0 & 0 & 0 & \hat{b}_z & -\hat{b}_y & 0 & -\hat{c}_z & \hat{c}_y \\ 0 & 0 & 0 & -\hat{b}_z & 0 & \hat{b}_x & \hat{c}_z & 0 & -\hat{c}_x \\ 0 & 0 & 0 & \hat{b}_y & -\hat{b}_x & 0 & -\hat{c}_y & \hat{c}_x & 0 \\ \hat{a}_x & \hat{a}_y & \hat{a}_z & 0 & 0 & 0 & 0 & 0 & 0 \\ 0 & 0 & 0 & \hat{b}_x & \hat{b}_y & \hat{b}_z & 0 & 0 & 0 \\ 0 & 0 & 0 & 0 & 0 & 0 & \hat{c}_x & \hat{c}_y & \hat{c}_z \end{vmatrix} \cdot \begin{vmatrix} \omega_{Ax} \\ \omega_{Ay} \\ \omega_{Az} \\ \omega_{Bx} \\ \omega_{By} \\ \omega_{Bz} \\ \omega_{Cx} \\ \omega_{Cy} \\ \omega_{Cz} \end{vmatrix} = \begin{vmatrix} -\hat{A}_x & \hat{B}_x & 0 \\ -\hat{A}_y & \hat{B}_x & 0 \\ -\hat{A}_z & \hat{B}_x & 0 \\ 0 & -\hat{B}_x\hat{C}_x & \\ 0 & -\hat{B}_x\hat{C}_y & \\ 0 & -\hat{B}_x\hat{C}_z & \\ 0 & 0 & 0 \\ 0 & 0 & 0 \\ 0 & 0 & 0 \end{vmatrix} \cdot \begin{vmatrix} \dot{q}_1 \\ \dot{q}_2 \\ \dot{q}_3 \end{vmatrix} \quad (4)$$

Out of any singular configuration, the matrix multiplying the set of the legs' angular velocities can be inverted. Then the direct velocity problem is solved simply by expressing the velocity of the mobile platform, that with some algebraic manipulation let us write the Jacobian matrix of the 3-PUU:

$$\begin{vmatrix} \dot{P}_x \\ \dot{P}_y \\ \dot{P}_z \end{vmatrix} = \left| \frac{\hat{\mathbf{a}}\cdot\hat{\mathbf{A}}\cdot(\hat{\mathbf{c}}\times\hat{\mathbf{b}})\ \ \hat{\mathbf{b}}\cdot\hat{\mathbf{B}}\cdot(\hat{\mathbf{a}}\times\hat{\mathbf{c}})\ \ \hat{\mathbf{c}}\cdot\hat{\mathbf{C}}\cdot(\hat{\mathbf{a}}\times\hat{\mathbf{b}})}{\hat{\mathbf{a}}\cdot(\hat{\mathbf{c}}\times\hat{\mathbf{b}})} \right| \cdot \begin{vmatrix} \dot{q}_1 \\ \dot{q}_2 \\ \dot{q}_3 \end{vmatrix} \quad (5)$$

2.4. Inverse velocity analysis

The inversion of (5) relates the velocity of the mobile platform to the corresponding motions of the actuators:

$$\begin{vmatrix} \dot{q}_1 \\ \dot{q}_2 \\ \dot{q}_3 \end{vmatrix} = \begin{vmatrix} \frac{\hat{a}_x}{\hat{\mathbf{a}}\cdot\hat{\mathbf{A}}} & \frac{\hat{a}_y}{\hat{\mathbf{a}}\cdot\hat{\mathbf{A}}} & \frac{\hat{a}_z}{\hat{\mathbf{a}}\cdot\hat{\mathbf{A}}} \\ \frac{\hat{b}_x}{\hat{\mathbf{b}}\cdot\hat{\mathbf{B}}} & \frac{\hat{b}_y}{\hat{\mathbf{b}}\cdot\hat{\mathbf{B}}} & \frac{\hat{b}_z}{\hat{\mathbf{b}}\cdot\hat{\mathbf{B}}} \\ \frac{\hat{c}_x}{\hat{\mathbf{c}}\cdot\hat{\mathbf{C}}} & \frac{\hat{c}_y}{\hat{\mathbf{c}}\cdot\hat{\mathbf{C}}} & \frac{\hat{c}_z}{\hat{\mathbf{c}}\cdot\hat{\mathbf{C}}} \end{vmatrix} \cdot \begin{vmatrix} \dot{P}_x \\ \dot{P}_y \\ \dot{P}_z \end{vmatrix}. \quad (6)$$

2.5. Acceleration analysis

Similarly to the velocity problem, a two-step algorithm is required. Firstly, we derive the linear system (4) and solve it to find the unknown angular accelerations of legs. With this information we obtain the acceleration of the

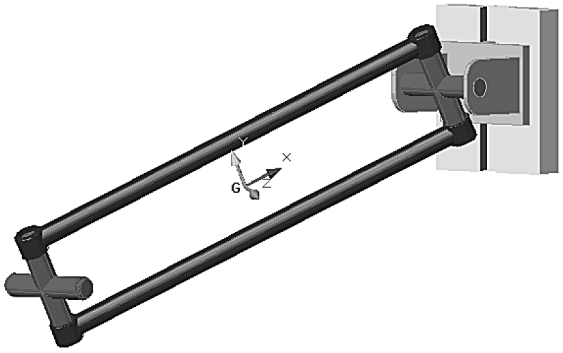

Fig. 4. A strut and its principal inertial axes.

mobile platform and write the omeomorphism represented by $\dot{J}$ in equation (7).

$$\ddot{\mathbf{P}} = J(\mathbf{q})\ddot{\mathbf{q}} + \dot{J}(\dot{\mathbf{q}},\mathbf{q}). \tag{7}$$

3. THE DYNAMIC MODEL

The Eulero-Newton approach is used for describing the inverse dynamic model of the generic 3-PUU class robotic platform in order to provide a tool useful either for the mechanical design both or control purposes.

This intention justifies the rather bulky approach to the kinematical analysis, that nevertheless delivers with a little effort the linear and angular differential terms for the three legs, thought as spread-mass bodies: by this way it is possible to quantify the static and dynamic loads that they undergo and forecast their stress status.

3.1. Balance of forces and torques acting on a leg

The fixed frame bears the orthogonal components of the upper universal joints' reactions $\mathbf{F}_A$, $\mathbf{F}_B$ and $\mathbf{F}_C$ to the prismatic pairs, while the set of $\boldsymbol{\tau}$ spread by linear motors balances the components acting along their directions. Furthermore the gravitational and inertial effects on the slides have to be considered:

$$\boldsymbol{\tau} = m_S \cdot \left(\ddot{\mathbf{q}} - \begin{vmatrix} \hat{\mathbf{A}}\cdot\mathbf{g} \\ \hat{\mathbf{B}}\cdot\mathbf{g} \\ \hat{\mathbf{C}}\cdot\mathbf{g} \end{vmatrix} \right) - \begin{vmatrix} R_{A3}\cdot\mathbf{F}_A \\ R_{B3}\cdot\mathbf{F}_B \\ R_{C3}\cdot\mathbf{F}_C \end{vmatrix}, \tag{8}$$

where the matrices R_A, R_B, R_C, whose columns are the Cartesian components of $\hat{\mathbf{A}}$, $\hat{\mathbf{B}}$, $\hat{\mathbf{C}}$, rotate the world reference system to a local frame with the *z*-axis laying along the sliding directions. The reactions on upper universal joints are made up of a component aligned with the linked strut and a normal one. If one considers leg "A" they are respectively $\mathbf{F}_{axA}$ and $\mathbf{F}_{nA}$. The second one appears in the balance of momenta around the pole **a** [6]:

$$\mathbf{F}_{nA}\times(\mathbf{a}-\mathbf{A}) = \frac{1}{2}m_L\cdot(\ddot{\mathbf{G}}-\mathbf{g})\times(\mathbf{a}-\mathbf{A}) + {}^{OXYZ}I_A\cdot\dot{\boldsymbol{\omega}}_A. \tag{9}$$

The attention has to be paid on the expression of ${}^{OXYZ}I_A$, that comes from ${}^{ZGxyz}I_A$, the diagonal inertia tensor in the principal inertial local reference system **Gxyz** (Fig. 4) with the simple relation:

$${}^{OXYZ}I_A = {}^{OXYZ}_{Gxyz}R_A \cdot {}^{Gxyz}I_A \cdot {}^{OXYZ}_{Gxyz}R_A^T. \tag{10}$$

The $\mathbf{F}_{na}$ component on the lower universal joint balances those forces that are normal to the leg:

$$\mathbf{F}_{na} + \mathbf{F}_{nA} = m_L[(\ddot{\mathbf{G}}_A - \mathbf{g}) - (\ddot{\mathbf{G}}_A - \mathbf{g})\cdot\hat{\mathbf{a}}\cdot\hat{\mathbf{a}}], \tag{11}$$

The axial components $\mathbf{F}_{axA}$ and $\boldsymbol{F}_{axa}$ on the upper and lower universal joints balance the components of the inertial and gravitational forces aligned with the strut;

$$\mathbf{F}_{axA} = \mathbf{F}_{axa} + m_L(\ddot{\mathbf{G}}_A - \mathbf{g})\cdot\hat{\mathbf{a}}. \tag{12}$$

J_p is similar to the Jacobian in (5), and by its trasposal the total force $\boldsymbol{F}_{tot}$ on the end-effector is decomposed along directions $\hat{\mathbf{a}}$, $\hat{\mathbf{b}}$, $\hat{\mathbf{c}}$. $\boldsymbol{F}_{tot}$ sums the applied load to the gravitational and inertial effects on the mobile platform and the components of constraint forces exerted by the lower Hooke's joints that are normal to the legs. As a matter of facts the axial components of forces on struts have the following expression:

$$\begin{vmatrix} F_{axa} \\ F_{axb} \\ F_{axc} \end{vmatrix} = J_P^{\mathrm{T}}\cdot\mathbf{F}_{tot} = \left| \frac{\hat{\mathbf{c}}\times\hat{\mathbf{b}} \;\; \hat{\mathbf{a}}\times\hat{\mathbf{c}} \;\; \hat{\mathbf{a}}\times\hat{\mathbf{b}}}{\hat{\mathbf{a}}\cdot(\hat{\mathbf{c}}\times\hat{\mathbf{b}})} \right|^{\mathrm{T}} \cdot\mathbf{F}_{tot}. \tag{13}$$

The equations (9, 11, 12) and (13) are useful for analyzing the stresses and deformations on components. Nevertheless some laborious algebraic manipulations are needed for putting them in a well known and handily fashion, that is common in the control practice:

$$\boldsymbol{\tau} = M(\mathbf{q})\ddot{\mathbf{q}} + N(\mathbf{q},\dot{\mathbf{q}}) + G(\mathbf{q}). \tag{13}$$

4. VERIFICATION OF THE MODEL

The CAE simulation with the multibody software MSC visualNastran® 4D has been used to check the correctness of both the kinematical and dynamic models. In the first case, several laws of motion in the Cartesian space were assigned to the mobile platform and the measured displacement of the sliders was compared to the corresponding ones calculated with Matlab (Fig. 5).

The obtained displacement values were subsequently exported to a properly formatted text files, and used as inputs to drive the elongation of the telescopic rods by which visualNastran represents the linear actuators.

Table 1

Geometrical features of the modelled robot

Radius of the fixed platform	0.5 m
Radius of the mobile platform	0.12 m
Length of the struts	0.85 m
Slope of the branches of the fixed frame	60°

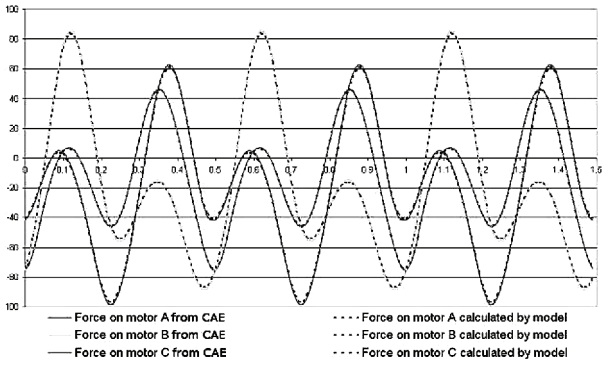

Fig. 5. Comparison between model and CAE model.

By this way in a yet kinematical simulation, the software allow to record the tensile stresses on the drives and compare them with the results of the dynamic model.

Being all parameters involved in the analytic investigation re-configurable, the verification of a certain architecture ensures that robot with any set of geometrical and inertial values are described properly.

5. STIFFNESS ANALYSIS

The two main factors for the mechanism's compliance, namely the deformations of the struts in response of axial solicitations and the finite stiffness of the actuation devices were thought as uncoupled and thus modeled as the serial arrangement of two linear springs. The bending of the legs was indeed neglected.

The search for the quasi-isotropic stiffness condition lead to adopt as a condition number the ratio between the maximum and minimum eigenvalue of the product of the Jacobian matrix by its trasposal, that's to say the ratio between the semi-axes of the resistance ellipsoid. A typical limit value of this ratio is 5 [3].

$$C_n = \sqrt{\frac{\lambda_{\max}(JJ^{\mathrm{T}})}{\lambda_{\min}(JJ^{\mathrm{T}})}}. \qquad (14)$$

The physical meaning of this index is related to the ratio between the forces along the directions of maximum and minimum stiffness capable to provoke a tool platform's threshold deflection δ. By this reason it is interesting to map throughout the workspace the values of minimum forces associated to a certain δ (See Fig. 6). Such values are obtained as the solution of the Lagrange's multiplier:

$$L(\Delta P, \lambda) = \Delta P^{\mathrm{T}} K^2 \Delta P - \lambda(\Delta P^{\mathrm{T}} \Delta P - \delta^2) \qquad (15)$$

In this case K includes both the stiffness of linear actuators ($k_q \approx 25$ N/μm) and the stiffness of legs, whose cross section's area is *A*, by mean of the matrix J_p:

$$K = \left(\frac{EA}{L} \cdot J_P^{\mathrm{T}} J_P + \frac{1}{k_q} \cdot J^{\mathrm{T}} J \right)^{-1}. \qquad (16)$$

The overall characterization of the operative space of 3-PUU robotic platforms with high and low slope of the fixed side columns in terms of isotropy and stiffness is resumed in the Table 2. There is substantial agreement with the existing literature [3, 4].

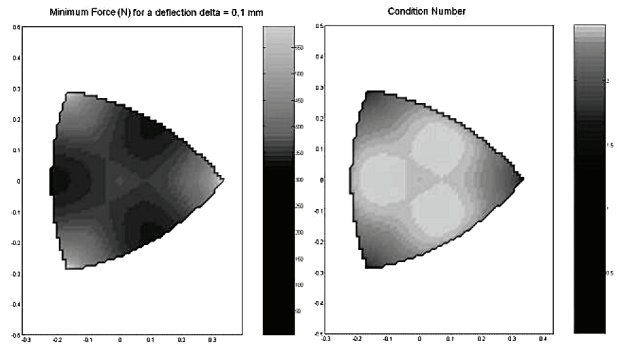

Fig. 6. An example of stiffness map (ϕ = 72°, $|\mathbf{OV_0}|$ = 0.9 m).

Table 2

Overall influence of the slope of the fixed columns

	Low sloped guides	**High sloped guides**
Shape of workspac	Wide, singularities reduce performance when the tool is close to fixed platform. Poor vertical extent	Narrow bur very tall: It consist of two parts divided by an highly singular region.
Isotropy	Scarce when tool is close to fixed platform, good elsewhere	High, but suffering from parallel singularities
Mean stiffness	Mechanical gain raises heavily with distance from fixed platform	Mechanical gain raises quite with distance from fixed platform
Notes	Optimal in quasi planar applications	Fixed frame may interfere

6. CONCLUSIONS

A parametric mathematical model of the 3-PUU PKM, that seems to be much promising for high speed and precise working has been presented. The dynamic inverse problem was solved with the Newton-Eulero approach, with the aim of providing a valuable tool for the structural design. The output generated by it agreed with the data collected on a CAE model very well. The stiffness of that class of parallel robots was investigates by mean of the mapping of two conditions numbers throughout the workspace. In a further development a multi-variable optimization study relying on both these algorithms will be propaedeutic to the construction of a physical prototype.

REFERENCES

[1] Callegari, M., Marzetti, P. (2004). *Kinematic characterisation of a 3-PUU parallel robot*, Proceeding of Intelligent Manipulation and Grasping, IMG04, pp. 377–382, Genova, Italy, June 30 – July 1, 2004.

[2] Company, O., Pierrot, F., Launay, F., Fioroni, C. (2000). *Modelling and preliminary design issues of a 3-axis parallel machine-tool*, Proceeding of PKM'00 International Conference on Parallel Kinematic Machines, pp. 14–23, Ann Arbor, Michigan, USA, September 13–15, 2000.

[3] Di Gregorio, R., Parenti-Castelli, V. (1998). *A translational 3 DOF parallel manipulator*, in: *Advances in Robot Kinematics: Analysis and Control*, J. Lenarcic and M. L. Husty Editors, Kluwer Academic Publisher, Dordrecht, Netherlands, pp. 49–58.

[4] Majou, F., Wenger, P., Chablat, D. (2001). *The design of parallel kinematic machine tools using kinetostatic performance criteria*, Proceeding of 3rd International Conference on Metal Cutting, Metz, France, 2001.

[5] Merlet, J. P. (2000). *Parallel Robots*, Kluwer Academic Publisher, Dordrecht, Netherlands.

[6] Harib, K., Srinivasan, K. (2003). *Kinematic and dynamic analysis of Stewart platform-based machine tool structures*, Robotica, pp. 541–554, Cambridge University Press.

Author:

Eng. Marco Principi, Ph.D. student in Artificial Intelligent Systems, Università Politecnica delle Marche, Department of Mechanics, Ancona, Italy, E-mail: m.principi@univpm.it